

# Crystal structure of a secondary vitamin D<sub>3</sub> binding site of milk $\beta$ -lactoglobulin

Ming-Chi Yang,<sup>1</sup> Hong-Hsiang Guan,<sup>2,3</sup> Ming-Yih Liu,<sup>2</sup> Yih-Hung Lin,<sup>2</sup> Jinn-Moon Yang,<sup>1</sup> Wen-Liang Chen,<sup>1</sup> Chun-Jung Chen,<sup>2,3\*</sup> and Simon J. T. Mao<sup>1,4\*</sup>

<sup>1</sup> Department of Biological Science and Technology, College of Biological Science and Technology, National Chiao Tung University, Taiwan, Republic of China

<sup>2</sup> Life Science Group, Research Division, National Synchrotron Radiation Research Center, Taiwan, Republic of China

<sup>3</sup> Department of Physics, Institute of Bioinformatics and Structural Biology, National Tsing Hua University, Taiwan, Republic of China

<sup>4</sup> Department of Biotechnology and Bioinformatics, Asian University, Taiwan, Republic of China

## ABSTRACT

*$\beta$ -lactoglobulin ( $\beta$ -LG), one of the most investigated proteins, is a major bovine milk protein with a predominantly  $\beta$  structure. The structural function of the only  $\alpha$ -helix with three turns at the C-terminus is unknown. Vitamin D<sub>3</sub> binds to the central calyx formed by the  $\beta$ -strands. Whether there are two vitamin D binding-sites in each  $\beta$ -LG molecule has been a subject of controversy. Here, we report a second vitamin D<sub>3</sub> binding site identified by synchrotron X-ray diffraction (at 2.4 Å resolution). In the central calyx binding mode, the aliphatic tail of vitamin D<sub>3</sub> clearly inserts into the binding cavity, where the 3-OH group of vitamin D<sub>3</sub> binds externally. The electron density map suggests that the 3-OH group interacts with the carbonyl of Lys-60 forming a hydrogen bond (2.97 Å). The second binding site, however, is near the surface at the C-terminus (residues 136–149) containing part of an  $\alpha$ -helix and a  $\beta$ -strand I with 17.91 Å in length, while the span of vitamin D<sub>3</sub> is about 12.51 Å. A remarkable feature of the second exosite is that it combines an amphipathic  $\alpha$ -helix providing nonpolar residues (Phe-136, Ala-139, and Leu-140) and a  $\beta$ -strand providing a nonpolar (Ile-147) and a buried polar residue (Arg-148). They are linked by a hydrophobic loop (Ala-142, Leu-143, Pro-144, and Met-145). Thus, the binding pocket furnishes strong hydrophobic force to stabilize vitamin D<sub>3</sub> binding. This finding provides a new insight into the interaction between vitamin D<sub>3</sub> and  $\beta$ -LG, in which the exosite may provide another route for the transport of vitamin D<sub>3</sub> in vitamin D<sub>3</sub> fortified dairy products. Atomic coordinates for the crystal structure of  $\beta$ -LG-vitamin D<sub>3</sub> complex described in this work have been deposited in the PDB (access code 2GJ5).*

Proteins 2008; 71:1197–1210.  
© 2007 Wiley-Liss, Inc.

**Key words:** fluorescence ligand binding assay; crystallography; localized alternative vitamin D binding site; thermal denaturation; amphipathic helix.

## INTRODUCTION

Bovine  $\beta$ -lactoglobulin ( $\beta$ -LG) is a major whey protein in milk to an extent of about 50%.<sup>1</sup> Because of its thermally unstable and molten-globule nature,  $\beta$ -LG has been studied extensively for its physical and biochemical properties in the past 40 years.<sup>2–6</sup> Although the biological functions of the protein still remain elusive, some essential functions of  $\beta$ -LG, such as cholesterol lowering, modulation of immune system, transport of retinol, fatty acid, and vitamin D,<sup>7–9</sup> and prevention of oxidative stress,<sup>10,11</sup> have been reported.

Several crystal forms of bovine  $\beta$ -LG have been described.<sup>12–21</sup> Of these, lattices X and Z (Space group *P*1 and *P*<sub>3</sub>21) have been investigated at a low resolution.<sup>14</sup> A high resolution study of another crystal form, lattice Y, has yielded a chain trace and a preliminary model.<sup>14</sup> The overall folding turns out to be remarkably similar to that of the human plasma retinol binding protein<sup>15,16,22,23</sup> and human tear lipocalin,<sup>24</sup> known as members of the lipocalin superfamily. As shown in Figure 1(A),  $\beta$ -LG comprises of 162 amino acid residues with two disulfide linkages and one free cysteine. It has predominantly a  $\beta$ -sheet configuration containing nine antiparallel  $\beta$ -strands from A to I.<sup>18,19,25</sup> Topographically,  $\beta$ -strands A–D form one surface of the barrel (calyx), whereas strands E–H form the other.

The only  $\alpha$ -helical structure with three turns is at the COOH-terminus (residues 130–141), which is followed by a  $\beta$ -strand I lying on the outer surface of the calyx.<sup>26</sup> The

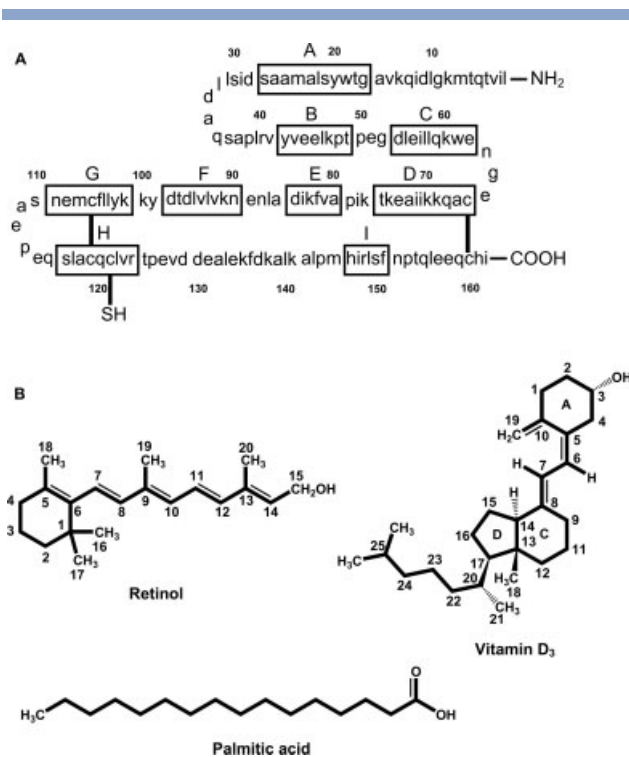
Grant sponsor: National Science Council (NSC); Grant numbers: 92-2313-B-009-002, 93-2313-B009-002, 94-2313-B-009-001, 95-2313-B-009-001, 94-2321-B-213-001; Grant sponsor: National Synchrotron Radiation Research Center (NSRRC); Grant numbers: 944RSB02, 954RSB02.

\*Correspondence to: Simon J. T. Mao, Department and College of Biological Science and Technology, National Chiao Tung University, 75 Po-Ai Street, Hsinchu, 30068 Taiwan, ROC. E-mail: mao1010@ms7.hinet.net and Chun-Jung Chen, Life Science Group, Research Division, National Synchrotron Radiation Research Center, 101 Hsin-Ann Road, Hsinchu, 30076 Taiwan, ROC. E-mail: cjchen@nsrrc.org.tw

Received 13 April 2007; Revised 16 August 2007; Accepted 22 August 2007

Published online 14 November 2007 in Wiley InterScience (www.interscience.wiley.com).

DOI: 10.1002/prot.21811

**Figure 1**

*Amino acid sequence of  $\beta$ -LG and chemical structure of its binding ligands. (A)  $\beta$ -LG is consisted of 162 amino acids with nine  $\beta$ -sheet strands (A-I) and one  $\alpha$ -helix at the COOH-terminus. There are two disulfide linkages located between strand D and COOH-terminus (Cys-66 and Cys-160) and between strands G and H (Cys-106 and Cys-119), with a free buried thio-group at Cys-121.  $\alpha$ -helix with three turns is located between residues 130 and 141 (in light gray). (B) Chemical structure of retinol, palmitic acid, and vitamin D<sub>3</sub>.*

structural and functional relationship of this helical region is not yet clearly defined. Studies on the crystal structure of  $\beta$ -LG-retinol complex at 2.5 Å resolution by Monaco *et al.* have pointed out that there is a surface pocket consisting of almost completely hydrophobic residues near the helical region.<sup>16</sup>

The remarkable ability of the calyx to bind hydrophobic molecules, such as retinol, fatty acids, and vitamin D [Fig. 1(B)],<sup>27–29</sup> has recently been reviewed by Kontopidis *et al.*<sup>9</sup> It seems clear that the binding of fatty acid, retinol, and vitamin D is within the central calyx of the protein; however, the existence of a second ligand binding site beyond the calyx is a matter of controversy.<sup>9</sup> Interestingly, an early study has suggested that a hydrophobic pocket, formed by the  $\alpha$ -helix and the surface of the barrel, also exists.<sup>16</sup> This surface pocket, limited by Phe-136 and followed by residues 139–143 (Ala-Leu-Lys-Ala-Leu), has been suspected to potentially bind retinol;<sup>16</sup> however, later studies by X-ray diffraction did not reveal that retinol could occupy this site.<sup>9,29</sup> Using *cis*-parinaric acid as a ligand, Dufour *et al.*<sup>30</sup> have suggested that this ligand is bound in this hydrophobic pocket. It

remains unclear what type of ligands may interact with this surface site. The binding of vitamin D to  $\beta$ -LG is also controversial.<sup>9,31</sup> It has been postulated that there is another binding site, in addition to the calyx, for vitamin D based on the work of Swaisgood and de Wolf<sup>31–35</sup> by using biochemical binding assays. Subsequently, they also suggested that one vitamin D is bound in that hydrophobic site. Nevertheless, the location of the secondary binding site remote from the calyx has been implicated,<sup>15,16</sup> but has not yet been identified by the crystal structure of bovine  $\beta$ -LG with vitamin D<sub>2</sub>.<sup>9</sup>

Spectroscopic studies and thermodynamic analysis of the calorimetric signal have demonstrated that irreversible unfolding of the  $\beta$ -LG structure occurs upon thermal treatment above its transition temperature, 65–70°C.<sup>36</sup> Recently, we have shown that the conformational changes of  $\beta$ -LG are rapid and extensive at temperatures above the transition,<sup>5</sup> and  $\beta$ -strand D of the calyx is directly involved in the unfolding during the thermal denaturation.<sup>4</sup> As a result, the binding of palmitate or retinol to the central calyx is diminished. In the present study, we also demonstrated that the maximal binding ratios of vitamin D<sub>3</sub> to  $\beta$ -LG were 2:1, similar to that established by Wang *et al.*<sup>31</sup> Our next strategy was to denature the conformation of the calyx by heating at 100°C for 16 min; under this condition the calyx pocket was thermally “removed.” We then tested whether the thermally denatured  $\beta$ -LG was able to bind vitamin D<sub>3</sub>, palmitate, and retinol. Interestingly, only vitamin D<sub>3</sub> bound the heated  $\beta$ -LG and the binding ratio of vitamin D<sub>3</sub> to the heated  $\beta$ -LG was found to be 1:1. Thus, it suggests that there is a secondary site for vitamin D<sub>3</sub> binding, which is thermally independent. To confirm the hypothesis that a second vitamin D<sub>3</sub> binding site exists, we determined the crystal structure of  $\beta$ -LG-vitamin D<sub>3</sub> complex and attempted to identify, localize, and characterize such a site.

## MATERIALS AND METHODS

### Materials

$\beta$ -LG was purified from raw milk using saturated ammonium sulfate (40%) followed by a G-150 column chromatography of the upper fraction as described previously.<sup>3</sup> All-*trans* retinol, palmitic acid, vitamin D<sub>3</sub> (cholecalciferol), and *N*-acetyl-L-tryptophanamide were purchased from Sigma-Aldrich (St. Louis, MO).

### Ligand binding to $\beta$ -LG

$\beta$ -LG stock solution was prepared in 0.01M phosphate buffered solution, pH 8.0 (PB). Retinol, palmitate, and vitamin D<sub>3</sub> were prepared using absolute ethanol and purged with nitrogen and stored at –80°C in the dark. All the binding assays described below were conducted at

24°C. The ligand binding assay of  $\beta$ -LG was measured by fluorescence emission techniques similar to that previously described.<sup>4,31,32</sup> In general, the binding of retinol to  $\beta$ -LG was measured by extrinsic fluorescence emission of a retinol molecule at 470 nm using excitation at 287 nm, whereas binding of palmitate or vitamin D<sub>3</sub> to  $\beta$ -LG was measured by the fluorescence enhancement or quenching of Trp-19 of  $\beta$ -LG at 332 nm using excitation at 287 nm. Fluorescence spectra were recorded with a fluorescence spectrophotometer (Hitachi F-4500; Tokyo, Japan). For the titration experiment, 5  $\mu$ M of native  $\beta$ -LG was instantly incubated with various proportions of retinol or vitamin D<sub>3</sub> (0.625–25  $\mu$ M) at pH 8.0. For palmitate (2.5–100  $\mu$ M), 20  $\mu$ M of native  $\beta$ -LG was used. A solution of *N*-acetyl-L-tryptophanamide with an absorbance at 287 nm—equal to that of the protein—served as a blank. The change in fluorescence of this solution with titration caused by an inner filter effect was corrected as described by Cogan *et al.*<sup>37</sup> The change in fluorescence intensity at 332 nm or 470 nm was assumed to depend on the amount of protein-ligand complex, which allowed the calculation of *a*, the fraction of unoccupied ligand-binding sites on the protein:  $a = (F - F_{\text{sat}})/(F_0 - F_{\text{sat}})$ . Here *F* is the fluorescence intensity at a certain titration ratio, *F*<sub>sat</sub> is the corrected fluorescence intensity of  $\beta$ -LG solution with its sites saturated, and *F*<sub>0</sub> is the initial corrected fluorescence intensity. These data were then used to construct a plot of *P<sub>T</sub>a* versus *R<sub>T</sub>a*/(1 - *a*) according to the equation:  $P_{\text{T}}a = (1/n)[R_{\text{T}}a/(1 - a)] - K_{\text{d}}^{\text{app}}/n$ , where *P<sub>T</sub>* is the total protein concentration, *n* is the number of binding sites per molecule, *R<sub>T</sub>* is the total ligand concentration, and *K<sub>d</sub><sup>app</sup>* is the apparent dissociation constant.

To study the effect of pH on the binding capacity, native  $\beta$ -LG between 5 and 20  $\mu$ M was instantly incubated with retinol, vitamin D<sub>3</sub>, or palmitate between 5 and 20  $\mu$ M. To determine the effect of heat on the binding ability,  $\beta$ -LG was preheated at between 50 and 100°C for 15 s to 16 min and stopped using a 20°C water bath. The preheated  $\beta$ -LG was then incubated with retinol, palmitate, or vitamin D<sub>3</sub> at pH 8.0. The final concentration of ethanol in the reaction mixture was kept less than 3% (vol/vol) for all the experiments mentioned above. The ligand binding ability of  $\beta$ -LG was calculated as described previously.<sup>4,31</sup> For the titration curve experiment, the data were expressed as the percentage of emission of  $\beta$ -LG that had the maximal binding ratio. For the heat denaturation experiment, the data were expressed as the percentage relative to native  $\beta$ -LG. All the data were collected in triplicate determinations.

### Circular dichroism spectrum

For the circular dichroism (CD) spectral measurements, each sample (0.5 mg/mL) was heated in 20 mM Tris, pH 8.0.<sup>4,38</sup> The CD spectra were recorded on a

spectropolarimeter (Jasco-J715; Tokyo, Japan) at 24°C over wavelength ranges from 200 to 250 nm, and recorded at a scan speed of 20 nm/min. All spectra were measured twenty times in a cuvette with a path length of 1.0 mm. Each  $\beta$ -LG sample (100  $\mu$ L) was preheated at 50, 60, 70, 80, 90, and 100°C for 16 min and instantly stopped in a 20°C water bath before an immediate measurement.

### Crystallization

Purified  $\beta$ -LG was concentrated to 20 mg/mL in 20 mM Tris, pH 8.0. Vitamin D<sub>3</sub> stock solution made up as 50 mM in ethanol was added to  $\beta$ -LG solution to give a molar ratio of 3:1 and incubated for 3 h at 37°C. Precipitation immediately occurred when  $\beta$ -LG and vitamin D<sub>3</sub> were mixed, and the solution drops became clear on the slides after 3–4 days. Crystallization of the  $\beta$ -LG-vitamin D<sub>3</sub> complex was achieved using the hanging-drop vapor-diffusion method at 18°C with 2  $\mu$ L hanging drops containing equal amounts of  $\beta$ -LG-vitamin D<sub>3</sub> complex and a reservoir solution (0.1M HEPES containing 1.4M trisodium citrate dehydrate, pH 7.5). Crystals 0.1–0.2 mm long grew after 7 days.

### Crystallographic data collection and processing

The crystals were mounted on a Cryoloop (0.1–0.2 mm), dipped briefly in 20% glycerol as a cryoprotectant solution, and frozen in liquid nitrogen. X-ray diffraction data at 2.4 Å resolution were collected at 110 K using the synchrotron radiation on the beamlines BL12B2 at SPring-8 (Harima, Japan) and BL13B at NSRRRC (Hsinchu, Taiwan). The data were processed using the *HKL2000* program.<sup>39</sup> The crystals belong to the space group *P*<sub>3</sub><sub>2</sub><sub>1</sub> with unit cell dimensions of *a* = *b* = 53.78 Å and *c* = 111.573 Å. There is one molecule per asymmetric unit according to an estimated solvent content in a reasonable region. Details of the data statistics are given in a table in the text.

### Crystal structure determination and refinement

The structure of the  $\beta$ -LG-vitamin D<sub>3</sub> was determined by molecular replacement<sup>40</sup> as implemented in *CNS v1.1*<sup>41</sup> using the crystal structure of bovine  $\beta$ -LG (PDB code 2BLG)<sup>18</sup> as a search model. The  $\beta$ -LG molecule was located in the asymmetric unit after rotation and translation function searches. All refinement procedures were performed using *CNS v1.1*. The composite omitted electron density maps with coefficients  $|2F_o - F_c|$  were calculated and visualized using *O v7.0*,<sup>42</sup> and the model was rebuilt and adjusted iteratively as required. Throughout the refinement, a random selection (8%) of the data was placed aside as a “free data set,” and the model was

refined against the rest of the data with  $F \geq 0$  as a working set.<sup>43–45</sup> The monomer protein model was initially refined by rigid-body refinement using the data from 15.0 to 3.0 Å resolution, for which the group temperature  $B$  values were first restrained at 20 Å<sup>2</sup>. This refinement was followed by simulated annealing using a slow cooling protocol with a starting temperature of 2500 K, provided in *CNS*, applied to all data between 15.0 and 2.4 Å. The bulk solvent correction was then applied, and group  $B$  factors were adjusted. After several cycles of positional and grouped  $B$  factor refinement interspersed with interactive modeling, the  $R$ -factor for the  $\beta$ -LG-vitamin D<sub>3</sub> complex decreased to about 28% with the  $R_{\text{free}}$  around 36%. Two elongated extra electron densities with one  $\beta$ -LG molecule were clearly visible and recognized as the vitamin D<sub>3</sub> in  $\sigma_A$ -weighted  $|F_o - F_c|$  difference maps. Two vitamin D<sub>3</sub> molecules were then adjusted and well fitted into the density map. The refinement then proceeded with another cycle of simulated annealing with a slow cooling, starting at a temperature of 1000 K. The vitamin D<sub>3</sub> molecules were adjusted iteratively according to the omitted electron density maps. Finally, water molecules were added using the program *CNS v1.1*.

### Model validation

The final model of  $\beta$ -LG and vitamin D<sub>3</sub> complex contains 1272 nonhydrogen protein atoms for the monomer  $\beta$ -LG, 28 atoms for one vitamin D<sub>3</sub> molecule, and 38 water molecules. The refinement statistics are given in the text. The correctness of stereochemistry of the model was verified using *PROCHECK*.<sup>46</sup> The calculations of r.m.s. deviations from ideality<sup>47</sup> for bonds, angles, and dihedral and improper angles performed in *CNS* showed satisfactory stereochemistry. In a Ramachandran plot,<sup>48</sup> all main chain dihedral angles were in the most favored and additionally allowed regions except for Tyr-99.

### Coordinates

Atomic coordinates for the crystal structure of  $\beta$ -LG-vitamin D<sub>3</sub> complex described in this work have been deposited in the PDB (access code 2GJ5).

## RESULTS

### Binding of $\beta$ -LG to retinol, palmitate, and vitamin D<sub>3</sub>

Using the titration method previously established by Wang *et al.*,<sup>31,32</sup> we show that the maximal binding of vitamin D<sub>3</sub> with  $\beta$ -LG was achieved at a 2:1 ratio; whereas the binding for retinol or palmitate remained to be 1:1 (Fig. 2). This result is similar to that reported previously by Wang *et al.*<sup>31,32</sup> and tends to support a notion that  $\beta$ -LG binds two vitamin D<sub>3</sub> molecules. The

two possibilities for this result are either that  $\beta$ -LG has the same binding site for two vitamin D<sub>3</sub> molecules or it possesses two independent vitamin D<sub>3</sub> binding sites.

### Effect of pH on $\beta$ -LG binding to retinol, palmitate, and vitamin D<sub>3</sub>

It has been postulated that pH plays a crucial role in controlling the opening of the calyx to allow the entrance of  $\beta$ -LG ligands. At low pH or below the Tanford transition (about pH 6), the EF loop (the calyx cap) is closed, disallowing the binding of the ligands. To explore whether there is another vitamin D<sub>3</sub> binding site that may not be affected by the Tanford transition, we monitored the binding of vitamin D<sub>3</sub> at various pH while using retinol or palmitate as a reference. A notable transition of vitamin D<sub>3</sub> binding to  $\beta$ -LG was found to occur between pH 6.0 and 8.0 (Fig. 3), similar to that of retinol and palmitate. The binding to vitamin D<sub>3</sub> or palmitate was decreased to some extent at pH 9–10 (Fig. 3). This could be due to the protonated state of Lys-69 inside the calyx being neutralized at a high pH as suggested previously.<sup>4,29</sup> It is of interest to note that unlike retinol and palmitate;  $\beta$ -LG at a pH between 2 and 6 still retains about 35% of the maximal binding for vitamin D<sub>3</sub> [Fig. 3(C)]. The data imply that there is a possible secondary binding site for vitamin D<sub>3</sub> that is independent of the calyx.

### Effect of heating on $\beta$ -LG binding to retinol, palmitate, and vitamin D<sub>3</sub>

The pH titration experiment described above was unable to yield an accurate explanation of the existence of another binding site for vitamin D<sub>3</sub>. Our previous work showed that thermally denatured  $\beta$ -LG (heated to 100°C for 5 min) was unable to bind to retinol and palmitate because of the unfolding of the calyx.<sup>4</sup> In the next experiment, our strategy was to thermally “remove” the calyx and then test whether heated  $\beta$ -LG retained an activity allowing vitamin D<sub>3</sub> binding. Figure 4 shows a notable and sharp decrease in retinol, palmitate, and vitamin D<sub>3</sub> binding to  $\beta$ -LG heated between 70°C and 80°C over time. The change of binding is consistent to the molten-globule nature of  $\beta$ -LG, which correlates to its transition temperature.<sup>4</sup> At temperatures above 80°C, the protein lost its binding ability to retinol and palmitate in a time-dependent fashion, but it still retained 40% of the binding to vitamin D<sub>3</sub> even after being heated at 100°C for 16 min [Fig. 4(C)]. The heated  $\beta$ -LG (100°C for 16 min) was further titrated with the binding of vitamin D<sub>3</sub> in excess. Figure 4(D) reveals that there was about 42% of maximal binding of vitamin D<sub>3</sub> relative to that using native  $\beta$ -LG. There was no fluorescence change while titrating with retinol or palmitate (data not shown). Remarkably, a maximal stoichiometry of 1:1 was observed between the denatured  $\beta$ -LG and vitamin D<sub>3</sub>.

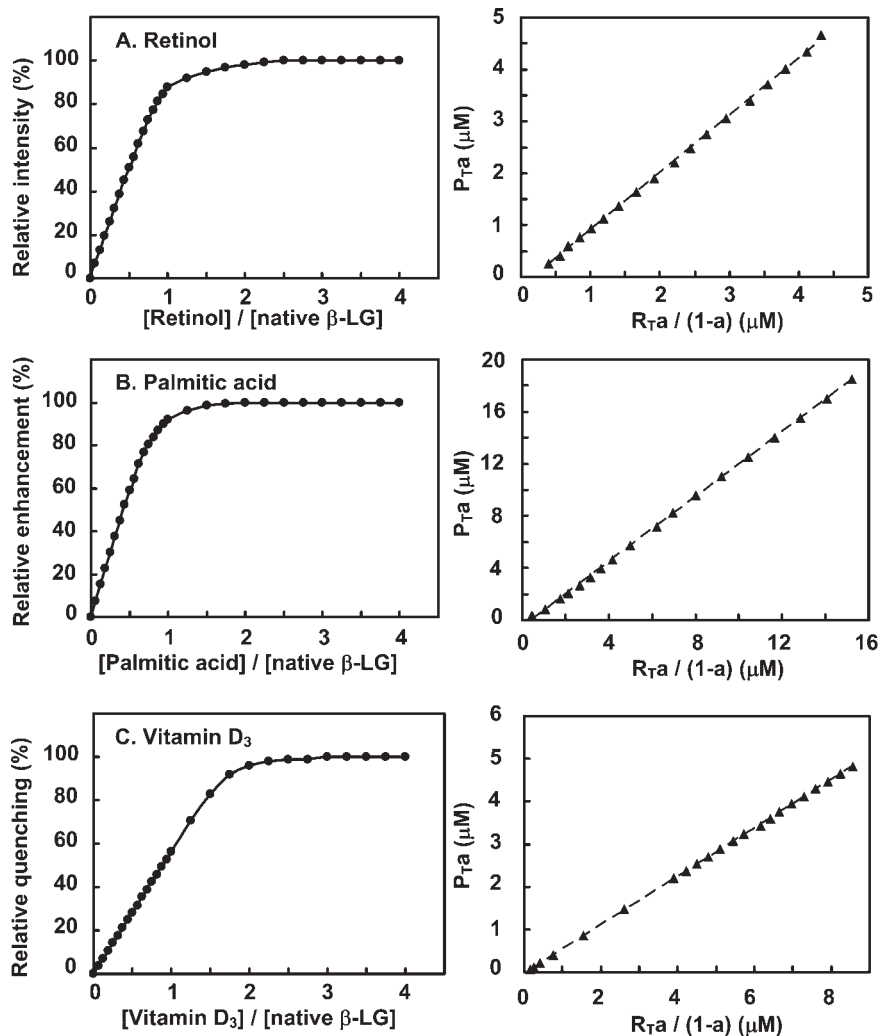


**Figure 2**

Binding ratio of  $\beta$ -LG with ligands. (A) Titration experiment for binding of  $\beta$ -LG to retinol measured at 470 nm with excitation at 287 nm (pH 8.0). Binding was determined by the enhancement of extrinsic fluorescence of retinol. (B, C) Titration experiment for binding of  $\beta$ -LG to palmitate and vitamin D<sub>3</sub> measured at 332 nm with excitation at 287 nm (pH 8.0). Binding was determined by the fluorescence enhancement (palmitate) and quenching (vitamin D<sub>3</sub>) of intrinsic fluorescence of  $\beta$ -LG. The maximal binding ratio of vitamin D<sub>3</sub> to  $\beta$ -LG is 2:1. Right panels:  $P_T$  = Total protein concentration,  $R_T$  = Total ligand concentration, and  $a$  = Fraction of unoccupied ligand sites on the protein. Each point represents the mean of triplicate determinations with an average of standard deviation (SD) less than 5–8% of the mean.

Thus, it suggests that a thermally stable site exists in  $\beta$ -LG to bind vitamin D<sub>3</sub>.

### Comparison of binding affinity of $\beta$ -LG to retinol, palmitate, and vitamin D<sub>3</sub>

We further determined the binding affinities of  $\beta$ -LG for retinol, palmitate, and vitamin D<sub>3</sub> using the method previously described by Wang *et al.*<sup>31,32</sup> The fluorescence data obtained for retinol, palmitate, and vitamin D<sub>3</sub> binding to native  $\beta$ -LG are shown in Figure 2 (right panels), while the vitamin D<sub>3</sub> binding to heated  $\beta$ -LG (100 °C for 16 min) is shown in Figure 4(D) (inserted panel).

Yielding values for the number of binding sites per molecule and apparent dissociation constant from the slope are listed in Table I. The binding affinity of vitamin D<sub>3</sub> to native  $\beta$ -LG using this method was about 5 nM ( $K_d^{app} = 4.74 \pm 0.37$  nM) and appears to be 5–10 times greater than that of retinol and palmitate. On the other hand, the binding affinity of vitamin D<sub>3</sub> to heated  $\beta$ -LG was attenuated at about 45 nM ( $K_d^{app} = 45.67 \pm 3.12$  nM), but is within the same order as that between native  $\beta$ -LG and retinol or palmitate. Because heating  $\beta$ -LG also induces the aggregation of  $\beta$ -LG,<sup>5</sup> the overall attenuated binding affinity of the “secondary site” indicates a structural change in the second binding site in heated  $\beta$ -LG.

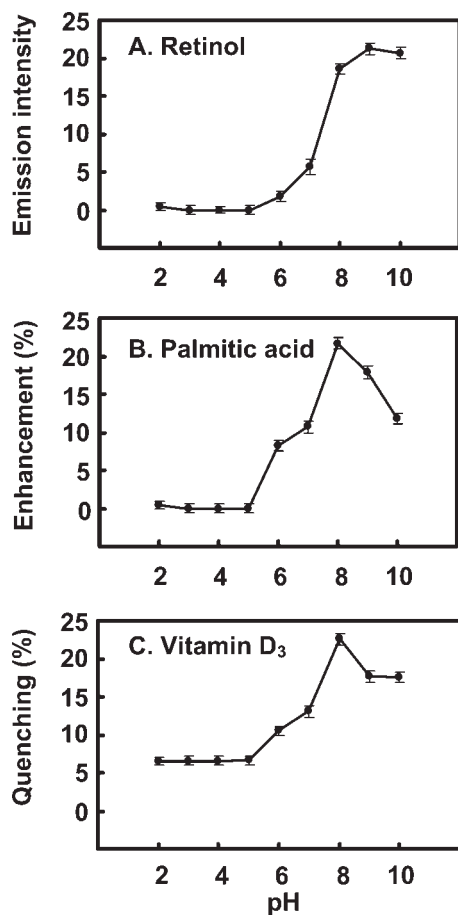


**Figure 3**

Effect of pH (Tanford transition) on  $\beta$ -LG binding with ligands. (A) Emission fluorescence of retinol. (B) Enhanced fluorescence of  $\beta$ -LG upon the binding of palmitate. (C) Quenched intrinsic fluorescence of  $\beta$ -LG upon the binding of vitamin D<sub>3</sub>. All the measurements are identical to that described in Figure 2. Each point represents the mean of triplicate determinations  $\pm$  SD.

Nevertheless, the data temptingly suggest that the putative second binding site is somewhat heat resistant.

### Overall crystal structure of $\beta$ -LG-vitamin D<sub>3</sub> complex

We have clarified that there are two vitamin D binding sites on  $\beta$ -LG according to ligand binding assay performed in solution. Protein crystallography was used to locate the secondary vitamin D binding site of  $\beta$ -LG. There are several crystal forms of bovine  $\beta$ -LG that have been well reported, including the triclinic (lattice X), orthorhombic (lattice Y), and trigonal (lattice Z) forms belonging to space groups  $P1$ ,  $C222_1$ , and  $P3_221$ , respectively.<sup>12–21</sup> The crystal of the  $\beta$ -LG-vitamin D<sub>3</sub> complex we obtained was found to be a trigonal (lattice Z) space group  $P3_221$  based on the data of 2.4 Å resolution. The final model comprised of 161 residues and its refinement

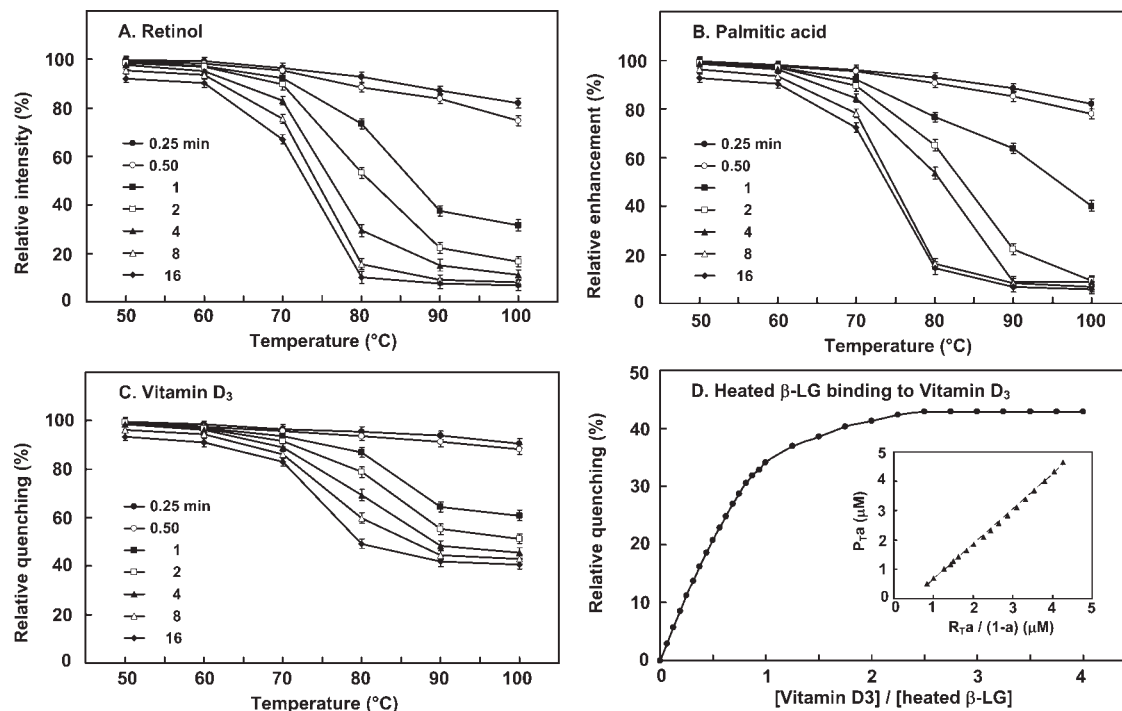
statistics of the complex are given in Table II. The discrepancy indices for  $R$  and  $R_{\text{free}}$  are 23.86% and 26.12%, respectively. The  $\beta$ -LG-vitamin D<sub>3</sub> complex possesses a well geometry similar to that reported by CNS<sup>27</sup> with a root-mean-square (r.m.s.) bond length and bond angle deviation from ideality 0.007 Å and 1.264°, respectively (Table II). A Ramachandran plot reveals that only one residue is in the disallowed regions (Tyr-99), which arises in most of the lipocalin family as a result of the  $\gamma$ -turn associated with the sequence “TDY” (residues 97–99). The average temperature factor for all protein atoms is 55.02 Å<sup>2</sup>, which is considered to be inadequate for established crystallographic standards. This may be explained by  $\beta$ -LG having nearly 25% of the residues located around flexible surface loops and NH<sub>2</sub>- and COOH-terminal regions. Previously published statistics of  $\beta$ -LG complexes<sup>9,27,29</sup> show a  $B$ -factor range of 41.3–57.27 (Table III), which accommodates for the elevated values acquired in this study that seem to deviate from the norm.

The overall topology of  $\beta$ -LG is similar to that previously described<sup>15–19</sup> with a well-defined antiparallel  $\beta$ -sheet structure and flexible loops connecting the secondary structure elements. The loops AB, CD, EF, and GH are more flexible than the others, consistent with the observations from other reported crystal structures.<sup>15–19</sup> The EF loop that acts as a flap is in the open position of the central calyx, which is expected when vitamin D<sub>3</sub> is present.

Space-filling drawings of the  $\beta$ -LG-vitamin D<sub>3</sub> complex show that there are two domains for vitamin D<sub>3</sub> binding (Fig. 5). One vitamin D<sub>3</sub> molecule inserts almost perpendicularly into the calyx cavity as expected and is consistent to the previous reports.<sup>9,29</sup> The other binds to the surface near the COOH-terminus of  $\beta$ -LG (residues 136–149), including part of the  $\alpha$ -helix and  $\beta$ -strand I (Fig. 1) as shown in Figure 6. The  $B$ -factor for the vitamin D<sub>3</sub> molecules in the calyx and the second site are 39.19 and 46.90, respectively (Table II). Proximity of these values to the published data<sup>9,27,29</sup> reveals the rigidity of vitamin D<sub>3</sub> bound to  $\beta$ -LG (Table III). For the second site, vitamin D<sub>3</sub> is close to the surface of  $\beta$ -LG with 17.91 Å in length, while the span of vitamin D<sub>3</sub> is about 12.51 Å. Under this orientation, the A ring or the aliphatic tail following the C/D rings of vitamin D<sub>3</sub> interacts with the  $\beta$ -strand I or the  $\alpha$ -helix of  $\beta$ -LG, respectively (Fig. 6). We putatively defined this second vitamin D<sub>3</sub> binding site as an exosite.

Figure 6 depicts that the bulk of the electron density is sufficient to cover the entire extent of vitamin D<sub>3</sub> in the calyx (in stereo view) as well as that in the exosite. The aliphatic tail of vitamin D<sub>3</sub> (C17–27) is oriented inside the calyx with the 3-OH group of vitamin D<sub>3</sub> near the outside of the pocket.

Superimposing the current  $\beta$ -LG-vitamin D<sub>3</sub> and previously described  $\beta$ -LG models (PDB codes 1BSQ) in the

**Figure 4**

Effect of heating on  $\beta$ -LG binding with ligands. (A–C)  $\beta$ -LG was heated between 50 and 100°C for 15 s to 16 min before the addition of retinol, palmitate, and vitamin D<sub>3</sub>. (D) Titration curve of heated  $\beta$ -LG (100°C for 16 min) with vitamin D<sub>3</sub>. Only vitamin D<sub>3</sub>, but not retinol and palmitate, was able to bind denatured  $\beta$ -LG with a molar ratio of  $\sim$ 1:1. The data suggest that there is another thermally independent vitamin D<sub>3</sub> binding site, which is remote from the calyx pocket. Each point in panels A–C represents the mean of triplicate determinations  $\pm$  SD. While, each point in panel D represents the mean of triplicate determinations with a SD less than 5–8% of the mean.

region of the calyx [Fig. 7(A)] reveals that the movement of the external EF “gate loop” of  $\beta$ -LG-vitamin D<sub>3</sub> is quite similar to that of the  $\beta$ -LG-retinol complex<sup>18,29</sup> (data not shown). Some side chains, such as Lys-60, Glu-62, Phe-105, and Met-107, require significant reposition to make room for vitamin D<sub>3</sub> insertion into the calyx. The atoms of vitamin D<sub>3</sub> near or at the “mouth” of the calyx possess higher values of *B*-factors suggesting their higher mobility. Figure 7(B) depicts the distance of vitamin D<sub>3</sub> to the  $\beta$ -LG calyx. The shortest interaction distance is hydrogen bonding between the 3-OH group of vitamin D<sub>3</sub> and Lys-60 (2.97 Å) of  $\beta$ -LG; whereas the only hydrogen bond involving retinol binding is that to Glu-62.<sup>29</sup> Hydrophobic interaction and the distances between the carbons of vitamin D<sub>3</sub> and Pro-38, Leu-39, Val-41, Ile-71, Ala-86, Phe-105, and Met-107 of  $\beta$ -LG are also displayed.

With respect to the second binding site for vitamin D<sub>3</sub>, it appears that vitamin D<sub>3</sub> is bound to a surface pocket between the COOH-terminal  $\alpha$ -helix and  $\beta$ -strand I (residues 136–149). The current  $\beta$ -LG-vitamin D<sub>3</sub> and previously described native  $\beta$ -LG models in this region (PDB codes 1BSQ) are superimposed and shown in Figure 8(A). Notably, there is not much conforma-

tional change near the exosite of  $\beta$ -LG upon the vitamin D<sub>3</sub> binding. Figure 8(B) shows the distance between vitamin D<sub>3</sub> and the amino acids involved (Asp-137, Leu-140, Lys-141, Leu-143, Met-145, His-146, Ile-147, and Arg-148). Although some charged residues of the exosite are involved, their interaction with vitamin D<sub>3</sub> is mainly hydrophobic with the charged groups of  $\beta$ -LG sticking out of the pocket. The data suggest that the contact is via a hydrophobic interaction. There is no evidence that the hydroxyl group of vitamin D<sub>3</sub> interacts with  $\eta$ 1 N of Arg-148 as the distance (4.9 Å) is greater than that of

**Table I**

Apparent Dissociation Constants and Binding Ratio for Binding Ligands to Native or Heated  $\beta$ -LG

Ligand	Binding ratio (ligand/ $\beta$ -LG)	$K_d^{app}$ (10 <sup>-9</sup> M)
	$\bar{X} \pm SD$	$\bar{X} \pm SD$
Retinol with native $\beta$ -LG	0.908 $\pm$ 0.089	17.28 $\pm$ 1.62
Palmitate with native $\beta$ -LG	0.801 $\pm$ 0.072	44.03 $\pm$ 4.56
Vitamin D <sub>3</sub> with native $\beta$ -LG	1.761 $\pm$ 0.121	4.74 $\pm$ 0.37
heated $\beta$ -LG	0.835 $\pm$ 0.054	45.67 $\pm$ 3.12

**Table II**Data Collection and Refinement Statistics of  $\beta$ -LG-Vitamin D<sub>3</sub> Complex

<b>Data collection</b>	
Space group	<i>P</i> 3 <sub>2</sub> 21
Cell dimensions	
<i>a</i> , <i>b</i> , <i>c</i> (Å)	53.780, 53.780, 111.573
$\alpha$ , $\beta$ , $\gamma$ (°)	90, 90, 120
Resolution (Å)	30–2.4 (2.49–2.4)
<i>R</i> <sub>sym</sub>	0.034 (0.226)
$\langle I/\sigma \rangle$	43.3 (10.3)
Completeness (%)	98.5% (99.5%)
Redundancy	7.0
<b>Refinement</b>	
Resolution (Å)	15–2.4
No. of unique reflections	7422
<i>R</i> <sub>work</sub> / <i>R</i> <sub>free</sub>	23.86%/26.12%
No. of atoms	
Protein	1272
Ligand	56
Water	38
<i>B</i> -factors	
Protein	55.02
Ligand in calyx/exosite	39.19/46.90
Water	52.47
R.m.s. deviations	
Bond lengths (Å)	0.007
Bond angles (°)	1.264

hydrogen bonding (bond length less than 3.13 Å) [Fig. 8(B)].

Furthermore,  $\beta$ -LG is primarily oriented as a  $\beta$  structure (50%); the only  $\alpha$ -helix region of  $\beta$ -LG consisting of three turns is located at the COOH-terminus between residues 130 and 141. Remarkably interesting, the  $\alpha$ -helix is arranged as amphipathic consisting of all the charged residues (Asp-130, Glu-131, Glu-134, Asp-137, Lys-138, and Lys-141) clustered at one face with hydrophobic or noncharged residues (Ala-132, Leu-133, Phe-136, Ala-139, and Leu-140) at another face without an exception [Fig. 9(A)]. A remarkable feature is that the exosite is comprised of an amphipathic  $\alpha$ -helix providing hydrophobic residues (Phe-136, Ala-139, and Leu-140) at one side and a  $\beta$ -strand providing a hydrophobic Ile-147 and a backbone His-146 at the other side [Fig. 9(B)]. These two sides are linked by a loop containing hydrophobic residues Ala-142, Leu-143, and Pro-144. Thus, the binding pocket provides a strong hydrophobic force to stabilize vitamin D<sub>3</sub> binding. The stereo view of such an interaction is also drawn in Figure 9(B), depicting the binding on the surface of  $\beta$ -LG. The carbons of vitamin

D<sub>3</sub> (*n* = 27 in total) close to the surface are C5, C8, C10, C13, C14, C15, C16, C17, C18, C19, C22, C24, C25, and C26 (*n* = 14). They are oriented toward the surface consistent with the analysis of Figure 5.

### CD spectrum analysis of heated $\beta$ -LG

In general, the CD spectrum at 222 nm is used for the calculation of the  $\alpha$ -helical content of a given protein. Because the  $\alpha$ -helix region of  $\beta$ -LG is located in the second binding site and heating  $\beta$ -LG retains ~40% of the maximal vitamin D<sub>3</sub> binding to the whole  $\beta$ -LG molecule, we monitored whether there were spectral changes of  $\beta$ -LG at 222 nm of  $\beta$ -LG upon heating at 50, 60, 70, 80, 90, and 100°C. Figure 10 reveals that there were no significant changes in spectra at 222 nm. As expected, the  $\beta$ -configuration was disordered at temperatures above 70°C, consistent with our previous observation.<sup>4</sup> Thus, it temptingly offers support that the proposed exosite is somewhat thermally stable.

## DISCUSSION

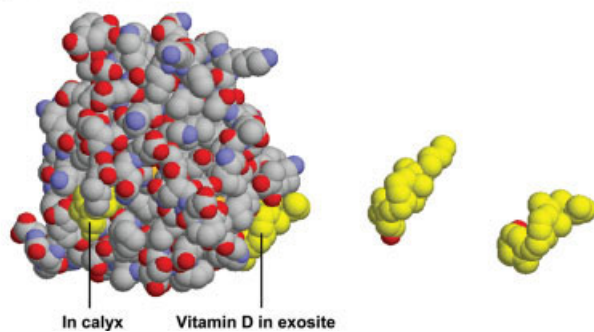
During the past 40 years,  $\beta$ -LG has been extensively studied for its biochemical properties, and an abundance of literature exists about its physicochemical nature.<sup>9</sup> Although the exact physiological functions of  $\beta$ -LG are not fully explored, one of its roles is to transport hydrophobic molecules, such as retinol, fatty acids, and vitamin D.<sup>49,50</sup> The active form of vitamin D is 1 $\alpha$ , 25(OH)<sub>2</sub> vitamin D<sub>3</sub>, which maintains calcium homeostasis and plays important roles on the immune system and prevents the growth and differentiation of cancer cells. Recent studies indicate that increased plasma vitamin D<sub>3</sub> concentrations are associated with decreased incidence of breast, ovarian, prostate and colorectal cancers,<sup>51</sup> and osteoporotic fractures.<sup>52</sup> The concentration of vitamin D<sub>3</sub> in plasma is about 80 nM. A double-blind placebo controlled study conducted in Europe indicated this level to be significantly reduced over the winter season (about 37%) due to the lack of exposure to sunlight.<sup>53</sup> However, drinking vitamin D<sub>3</sub> fortified milk (312 nM) significantly compensated the seasonal loss of vitamin D by greater than 50%. For this reason, it has been recommended that milk enriched with vitamin D<sub>3</sub> be provided in high-latitude European countries. Thus, we chose vitamin D<sub>3</sub>, instead of vitamin D<sub>2</sub>, to form a

**Table III**Mean *B*-Factor for  $\beta$ -LG Complexes with Ligands Extracted from Previously Published Papers

Ligand	Retinol	Retinoic acid	Palmitate	Cholesterol	Vitamin D <sub>2</sub>	Mercury	12-Bromododecanoic acid
Mean <i>B</i> -factor for protein atoms (Å <sup>2</sup> )	56.1	48.8	54.2	44.5	57.27	50.0	41.3
Mean <i>B</i> -factor for ligand atoms (Å <sup>2</sup> )	65.0	66.8	58.4	69.9	72.6	53.5	52.1
Mean <i>B</i> -factor for water molecules (Å <sup>2</sup> )	67.4	59.0	68.1	53.0	56.9	55.9	72.6



## Space-filling model

**Figure 5**

Structure of  $\beta$ -LG complexed with vitamin D<sub>3</sub> at 2.4 Å resolution. Space-filling drawing of  $\beta$ -LG-vitamin D<sub>3</sub> complex. Vitamin D<sub>3</sub> (colored in yellow) and  $\beta$ -LG are drawn based on our final refined model with carbon, oxygen, and nitrogen atoms depicted in gray, red, and blue, respectively. Sulfur molecules (in orange) are buried inside at this face. It demonstrates that there are two distinct vitamin D<sub>3</sub> binding sites on each  $\beta$ -LG molecule. One is penetrated inside the calyx (left) and the other is lying on the surface between the  $\alpha$ -helix and  $\beta$ -strand I at the COOH-terminus (residues 136–149) (right).

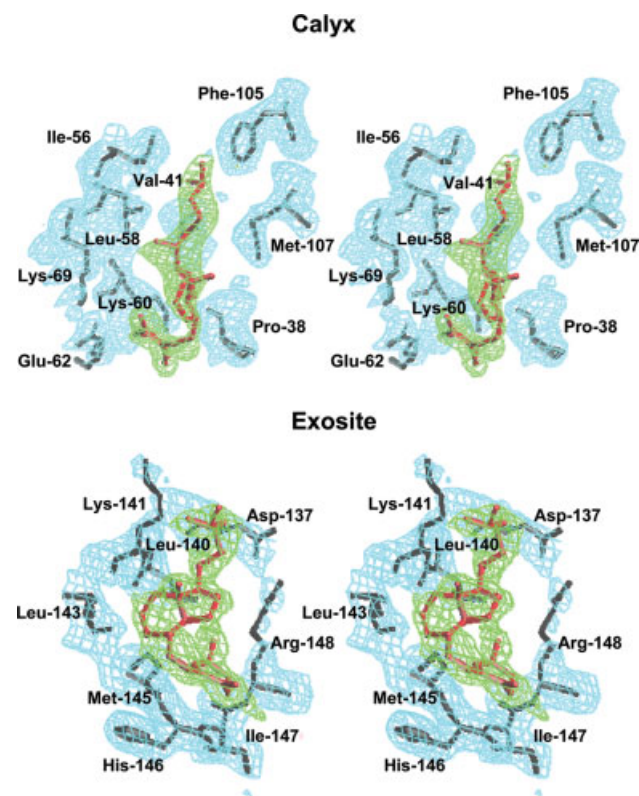
$\beta$ -LG-vitamin D<sub>3</sub> complex in this study. Structurally, the only difference of vitamin D<sub>3</sub> from D<sub>2</sub> is the latter being a double bond between the carbon positions 22 and 23 (Fig. 1). Despite the minor difference, their binding characteristics to  $\beta$ -LG are similar.<sup>31</sup> One additional goal in the present study is to test the possibility of binding vitamin D<sub>3</sub> to thermally denatured milk, which is often produced in the processing of milk.

With respect to the ligand binding of  $\beta$ -LG, many research groups<sup>28,31,32</sup> have shown that the stoichiometry for binding retinol or palmitate to  $\beta$ -LG is 1:1, and most experimental evidence points to the calyx of  $\beta$ -LG as the binding site for retinol and palmitate.<sup>29</sup> However, there remains a debate about the stoichiometry for vitamin D<sub>3</sub> binding being 1 or 2. Wang *et al.*<sup>31,34</sup> proposed that  $\beta$ -LG has another binding site for vitamin D in addition to the central calyx, but doubt has been raised based on crystallographic analysis.<sup>9,29</sup> In fact, the presence of a secondary site for ligand binding has been described and proposed for some time,<sup>16</sup> but the identity of a  $\beta$ -LG-ligand complex by an X-ray crystal structure has not been elucidated.<sup>9</sup>

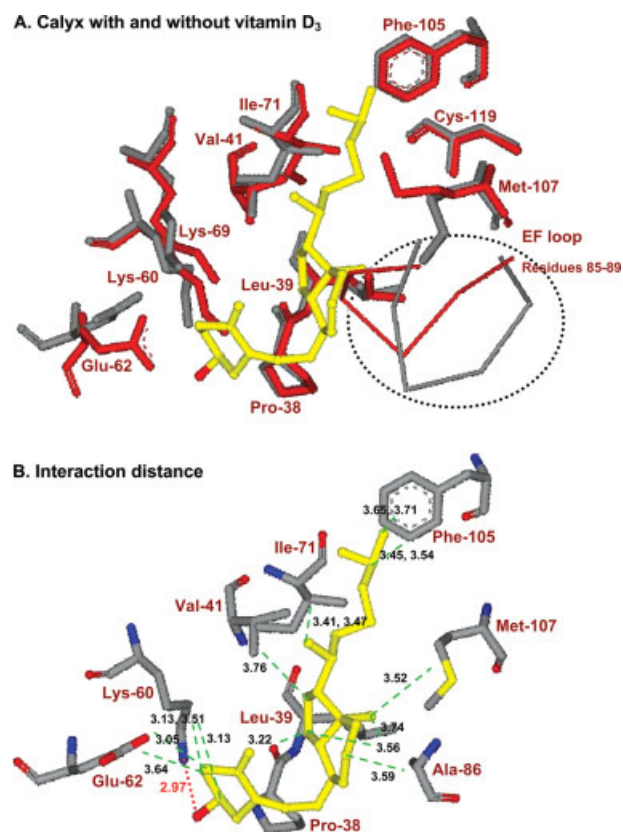
In the present work, using the method of extrinsic fluorescence emission and fluorescence enhancement and quenching established previously,<sup>4,31,32</sup> we show the maximal binding ratios of retinol or palmitate with  $\beta$ -LG to be 1:1, whereas it was 2:1 for that of vitamin D<sub>3</sub> (Fig. 2). The latter result is consistent to that reported by Wang *et al.*<sup>31,32</sup> It is worth mentioning that using the intrinsic fluorescence of Trp can give results that indicate significantly tighter ligand binding than other methods, especially equilibrium dialysis. This effect is particularly noticeable when the Trp fluorescence decreases with

ligand addition.<sup>9,35</sup> A recent review<sup>9</sup> suggests that a surface low-affinity binding site together with a central high-affinity binding site (calyx) would appear to satisfy most of the reported experimental observations. In brief, the diverse reports of more than a single binding site may be dependent on the method used.

In an attempt to resolve the controversy about an additional binding site for vitamin D<sub>3</sub>, we used several additional approaches involving structural change to study the interaction between vitamin D<sub>3</sub> and  $\beta$ -LG. First, it has been established that the EF loop acts as a gate over the calyx.<sup>9,18,29,54</sup> At a low pH, the loop is in a “closed” position, and the ligand binding into the calyx is inhibited. On the contrary, at a high pH above the Tanford transition, the loop is “open” allowing ligands to penetrate into the calyx.<sup>4,54,55</sup> We explored the binding ability between  $\beta$ -LG and vitamin D<sub>3</sub> at various pH. Similar to that of retinol and palmitate, the present study shows that there is a notable transition of vitamin D<sub>3</sub>

**Figure 6**

Electron density map around the calyx and the exosite of vitamin D<sub>3</sub>- $\beta$ -LG complex at 2.4 Å resolution. Final refined model together with the  $2F_{obs} - F_{calc}$  electron density show that the bulk of the electron density is sufficient to cover a vitamin D<sub>3</sub> molecule, both in the calyx (top) and the exosite (bottom). In the central calyx binding mode, the aliphatic tail of vitamin D<sub>3</sub> clearly inserts into the binding cavity, where the 3-OH group of vitamin D<sub>3</sub> binds externally. In exosite binding mode, vitamin D<sub>3</sub> interacts mostly with the hydrophobic moiety of the pocket.

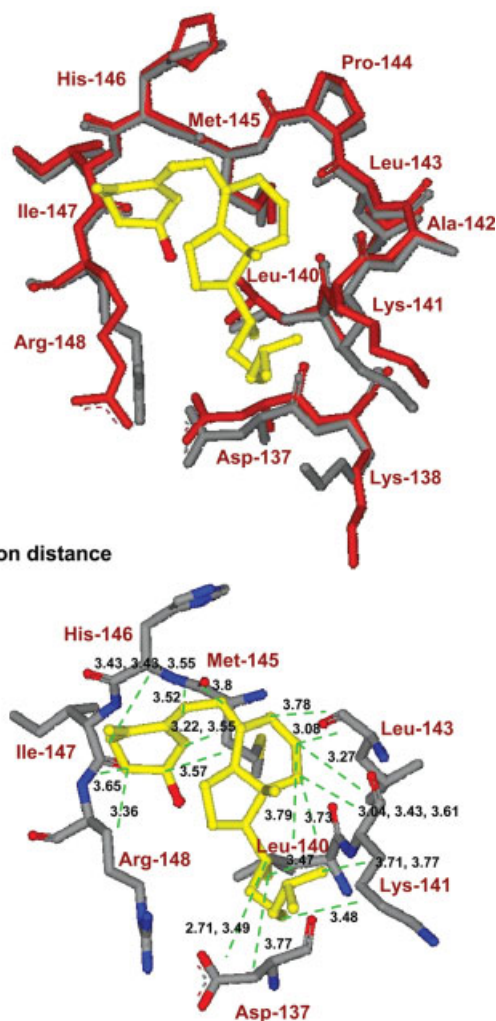
**Figure 7**

Superimposed structure of the calyx before and after binding of vitamin D<sub>3</sub> and a diagram showing their contacts less than 3.8 Å. (A) Superimposing the current model for vitamin D<sub>3</sub>-β-LG (colored in gray) with previously described native β-LG (in red) (PDB code 1BSQ) in the calyx shows that there is a significant repositioning of Glu-62 and Met-107 to make room for the ligand into the calyx. Notably, vitamin D<sub>3</sub> binding has resulted in a local conformational change by opening the EF loop as shown in a dotted circle (residues 85–89). Such conformational change in the loop is similar to the binding of retinol (data not shown). (B) The calyx of β-LG offers mainly hydrophobic interactions to vitamin D<sub>3</sub> binding (less than 3.8 Å). The shortest distance, 2.97 Å, is the hydrogen bond between the 3-OH group of vitamin D<sub>3</sub> and Lys-60 (dotted red). [Color figure can be viewed in the online issue, which is available at [www.interscience.wiley.com](http://www.interscience.wiley.com).]

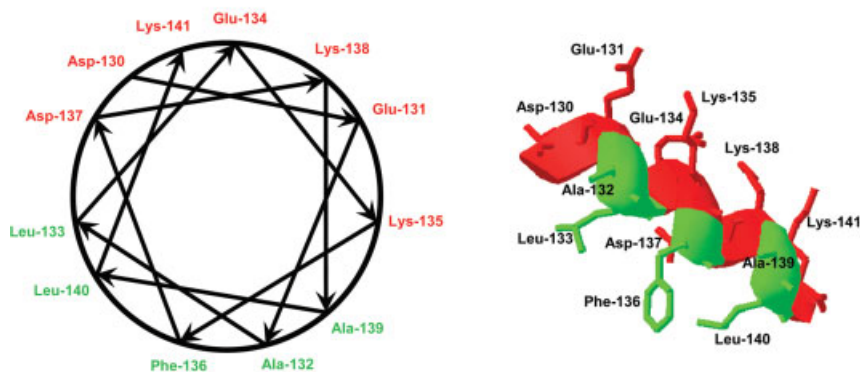
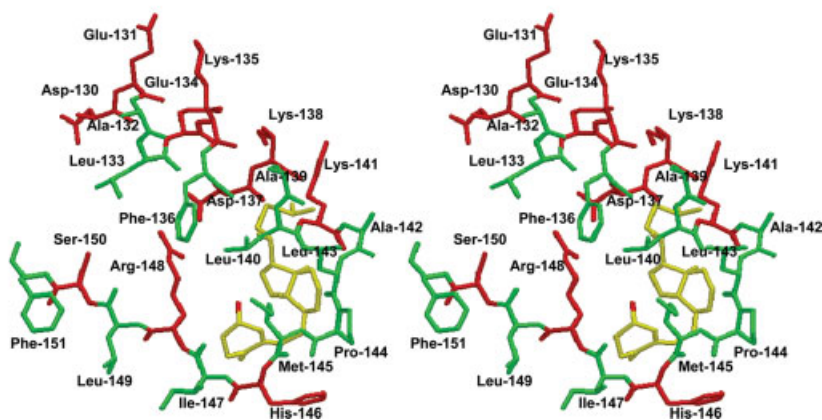
binding to the calyx of β-LG occurring between pH 6.0 and 8.0 (Fig. 3). Most interestingly, at pH between 2 and 6 we show vitamin D<sub>3</sub> interacting with β-LG (with about 35% of maximal binding ability), but not retinol and palmitate [Fig. 3(C)]. Because the EF loop is “closed” below the Tanford transition, such binding suggests the presence of another binding site for vitamin D<sub>3</sub>. Physiologically, such low pH binding could be essential, since β-LG is well known to be stable at low pH<sup>1,2</sup> and resistant to acid hydrolysis and protease digestion in the gastrointestinal tract.<sup>56,57</sup> Notably, the binding of vitamin D<sub>3</sub> or palmitate to β-LG was decreased to some extent at pH 9–10 (Fig. 3). One of the possible explanations is that the positively charged groups of lysine residues inside calyx are neutralized at pH above 8 resulting in a

weakening of the interaction with the carboxyl group of palmitate.<sup>4</sup>

Second, we have shown that the β-strand D of the calyx is directly involved in the thermal denaturation.<sup>4</sup> The conformational changes of β-LG were rapid, extensive, and irreversible upon heating over 70–80°C.<sup>5</sup> As a result, it completely diminishes the binding of palmitate and retinol. To test the hypothesis that there is a putative second binding site for vitamin D<sub>3</sub> located independently

**A. Exosite with and without vitamin D<sub>3</sub>****Figure 8**

Superimposed structure of the exosite before and after binding of vitamin D<sub>3</sub> and a diagram showing their contacts of less than 3.8 Å. (A) Superimposing the current model for vitamin D<sub>3</sub>-β-LG (colored in gray) with previously described native β-LG (in red) (PDB code 1BSQ) in the exosite reveals that the overall conformation is not substantially changed upon the binding of vitamin D<sub>3</sub>. (B) The exosite is near the surface of C-terminal α-helix and β-strand I, where the 3-OH group of vitamin D<sub>3</sub> does not apparently form hydrogen bonding with β-LG. [Color figure can be viewed in the online issue, which is available at [www.interscience.wiley.com](http://www.interscience.wiley.com).]

A. Amphipathic  $\alpha$ -helixB. Stereo view of vitamin D<sub>3</sub>-exosite complex

## Figure 9

Amphipathic helix of  $\beta$ -LG and its interaction with vitamin D<sub>3</sub>. (A) The only  $\alpha$ -helix region of  $\beta$ -LG is located between residues 130 and 141 (Fig. 1). Most interestingly, the  $\alpha$ -helix is oriented as amphipathic with all the charged residues clustered on one side without an exception. (B) The crystal structure reveals that the hydrophobic side of the  $\alpha$ -helix forms a stable hydrophobic pocket with  $\beta$ -strand I. They are linked by a hydrophobic loop (residues 142–145) and thus facilitate the binding to vitamin D<sub>3</sub>. The stereo view shows that part of vitamin D<sub>3</sub> is near the surface, particularly for the aliphatic tail, which is consistent with that depicted in Figure 5.

from the calyx, we thermally denatured the calyx (between 50 and 100°C) and then conducted the binding for retinol, palmitate, or vitamin D<sub>3</sub> over time (Fig. 4). It is of interest that only vitamin D<sub>3</sub> was able to bind to heated  $\beta$ -LG (at 100°C for 16 min) with a stoichiometry of almost 1:1, instead of 2:1 [Fig. 4(D)]. Our data suggests that the second binding site for vitamin D<sub>3</sub> is heat stable to some extent.

Third, analysis of the binding shows that the binding affinity between native  $\beta$ -LG and vitamin D<sub>3</sub> is relatively high within a nM range, about 10 times greater than palmitate and retinol (Table I). The result is almost the same as that of vitamin D<sub>2</sub> reported by Wang *et al.*,<sup>31</sup> but somewhat higher than the affinity reported for vitamin D<sub>3</sub>.<sup>31</sup> The reason contributing to such discrepancy remains elusive. One possibility may be due to the 5  $\mu$ M concentration (pH 8.0) of  $\beta$ -LG that we employed, while

Wang *et al.* used a 20  $\mu$ M concentration (pH 7.0) for a typical emission spectrum.<sup>34</sup> The other possibility may be due to the pH; the fluorescence of Trp may be affected by ionization of neighboring prototropic groups or by conformation changes due to the dimerization of the protein.<sup>2,34</sup> Nevertheless, the calculated affinity for vitamin D<sub>3</sub> ( $K_d^{\text{app}} = 45.67 \pm 3.12$  nM) to putative second or thermally stable binding site is about 10 times lower than that to native  $\beta$ -LG (calyx plus second site) (Table I). Thus, it seems to be consistent with the hypothesis proposed by Kontopidis *et al.*<sup>9</sup> that the central site (calyx) is a main binding site possessing a high affinity for most of the hydrophobic ligands, whereas the affinity for the secondary site is low. Ultimately, the secondary binding may depend on the nature of the ligands, such as their size, structure, and hydrophobicity. It would be of interest to further investigate other ligand bindings to

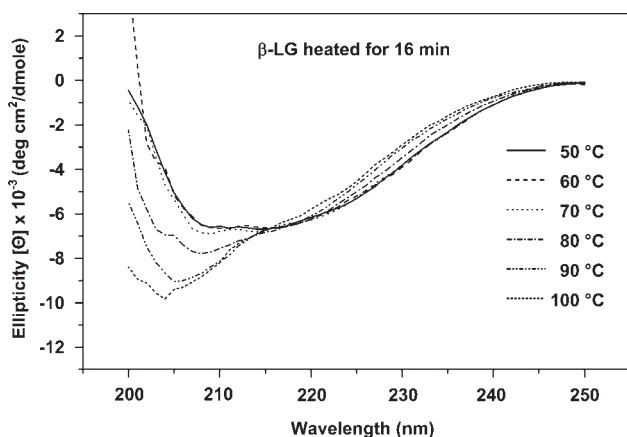


**Figure 10**

Circular dichroic spectra of native and heated  $\beta$ -LG.  $\beta$ -LG preheated between 50 and 100°C for 16 min was recorded by circular dichroism at a final concentration of 0.2 mg/mL. The  $\beta$ -structure of  $\beta$ -LG underwent disordering upon continuous heating as significant changes of ellipticity at 205–208 nm occurred above 80°C. The negative ellipticity at 222 nm, commonly a criteria for  $\alpha$ -helical structure, was identical between native and heated  $\beta$ -LG.

heated  $\beta$ -LG, although the calculation of binding affinity of heated  $\beta$ -LG is somewhat complicated owing to the formation of large  $\beta$ -LG polymers as mentioned (see Results).

Finally, to confirm our hypothesis that there exists a second vitamin D<sub>3</sub> binding site remote from the calyx, we used a synchrotron radiation X-ray to determine the crystal structure of the  $\beta$ -LG-vitamin D<sub>3</sub> complex. Our crystal of the complex is defined in trigonal (lattice Z) space group  $P3_221$ . This final model reveals that one vitamin D<sub>3</sub> molecule binds to the calyx (central internal binding-site) of  $\beta$ -LG and the other binds to the surface of  $\beta$ -LG between the  $\alpha$ -helix and  $\beta$ -strand I (external binding site; Fig. 5).

In the electron density map at 2.4 Å resolution, vitamin D<sub>3</sub> is well fitted into the bulk of electron density around the calyx or the exosite (Fig. 6). In central calyx binding mode, the aliphatic tail of vitamin D<sub>3</sub> clearly inserts into the binding cavity where the 3-OH group of vitamin D<sub>3</sub> binds externally. In an early report using vitamin D<sub>2</sub>,<sup>9</sup> the end that inserted into the calyx was not conclusively identified because the electron density was not enough to cover the entire ligand. It is not clear whether vitamin D<sub>3</sub> is superior to vitamin D<sub>2</sub> in binding to  $\beta$ -LG. The other difference is that in our study the 3-OH group of vitamin D<sub>3</sub> forms a hydrogen bond with the carbonyl of Lys-60 [Fig. 7(B)] instead of Lys-69 as proposed using vitamin D<sub>2</sub>.<sup>9</sup> Again, the electron density was not strong enough for the outer extremity of vitamin D<sub>2</sub> making the exact conclusion difficult. Another explanation is that there might be a significant difference in the orientation between vitamin D<sub>2</sub> and D<sub>3</sub>, although the

difference in chemical structure is subtle. Regardless, the vitamin D<sub>3</sub>- $\beta$ -LG binding mode is quite similar to that of retinol- $\beta$ -LG interaction over the calyx.<sup>29</sup> Pro-38, Leu-39, Val-41, Ile-71, Ala-86, Phe-105, and Met-107 are all involved in providing hydrophobic interactions with the displayed distance of less than 3.8 Å to the carbon backbone of vitamin D<sub>3</sub> [Fig. 7(B)].

In exosite binding mode, the vitamin D<sub>3</sub> molecule attaches at a pocket between the C-terminal  $\alpha$ -helix and  $\beta$ -strand I (Fig. 5). We specifically demonstrated that the exosite of  $\beta$ -LG provides a hydrophobic force to stabilize vitamin D<sub>3</sub> [Fig. 8(B)] and concluded that the exosite is located near the surface of the C-terminal  $\alpha$ -helix and  $\beta$ -strand I, where there is no strong evidence to show that the 3-OH group of vitamin D<sub>3</sub> is capable of interacting with  $\beta$ -LG [Fig. 8(B)]. A stereo view shown in Figure 9(B) reveals that part of the vitamin D<sub>3</sub> molecule is exposed toward the surface, consistent to that depicted in Figure 5. Although this second binding is located near the surface of  $\beta$ -LG, our data suggest that the binding affinity of vitamin D<sub>3</sub> to exosite is reasonably high and almost equivalent to that of retinol or palmitate to calyx (Table I). Apparently, vitamin D<sub>3</sub> interacts mostly with those hydrophobic amino acids within residues 136–149 with distances less than 3.8 Å [Fig. 8(B)]. The linking-loop residues 142–145 (Ala-Leu-Pro-Met) between the helix and strand I are all hydrophobic. With such an orientation, a hydrophobic pocket is constructed in facilitating the binding for vitamin D<sub>3</sub>. It is worth mentioning that this exosite is very similar to the surface hydrophobic site (mentioned and discussed above) that has been described by Monaco *et al.*<sup>16</sup> and proposed by Wang *et al.*<sup>31</sup>

It is of interest that the  $\alpha$ -helix involved in the exosite is typically amphipathic. This amphipathic region could be heat resistant as suggested from our binding experiment for vitamin D<sub>3</sub> and heated  $\beta$ -LG. A similar situation is seen in a typically amphipathic apolipoprotein A-I; its conformation and lipid binding properties are completely maintained upon heating over 100°C.<sup>58</sup> It might be worthwhile to study the crystal structure of the heated- $\beta$ -LG-vitamin D<sub>3</sub> complex to finally prove its heat resistance. Unfortunately, we are not able to crystallize such a complex at the present time. This could be due to the formation of multiple aggregated forms of  $\beta$ -LG upon heating.<sup>3–6</sup>

Vitamin D is found in only a few foods, such as fish oil, liver, milk, and eggs, in which milk is a major source for vitamin D in the diet. The level of vitamin D in bovine milk has been reported to be low. In many sophisticated food industries, processed milk, dry milk, margarine, and other dairy products are fortified with vitamin D<sub>3</sub> to a level of about 0.35  $\mu$ M. The concentration of  $\beta$ -LG in milk is about 270  $\mu$ M, providing a sufficient amount of  $\beta$ -LG to transport spiked vitamin D. It is of interest to point out that recent studies have demon-

strated that intact  $\beta$ -LG is acid resistant with a super permeability to cross the epithelium cells of the gastrointestinal tract.<sup>56,57</sup> Such a unique property of  $\beta$ -LG is worthy of consideration for transporting vitamin D in the milk.

There are two advantages for the presence of vitamin D<sub>3</sub> binding exosite in  $\beta$ -LG. First, central calyx of  $\beta$ -LG is thought to be primarily occupied by the fatty acid in milk.<sup>59</sup> The available exosite may provide another route for transporting the vitamin D. Second, many dairy products today are processed under excessive heat for the purpose of sterilization. The presence of a heat stable exosite may maintain the binding for vitamin D<sub>3</sub>.

Finally, since the putative exosite is located at the surface of  $\beta$ -LG, an approach using site-directed mutagenesis may eventually be served as to probe the structural and vitamin D binding relationship. The experiment is now in progress in our laboratory.

## ACKNOWLEDGMENTS

We are grateful to our colleagues, Dr. Yuch-Cheng Jean and Dr. Chun-Shiun Chao, and the supporting staffs for the technical assistance and discussion of the synchrotron radiation X-ray facility on data collection at BL13B1 of NSRRC, Taiwan, and Dr. Yu-San Huang and Dr. Kuan-Li Yu at BL12B2 of SPring-8, Japan. We also thank Dr. Su-Ying Wu of National Health Research Institutes (NHRI, Taiwan) for the useful discussion in preparing this manuscript.

## REFERENCES

1. Hambling SG, MacAlpine AS, Sawyer L. Beta-lactoglobulin. In: Fox PF, editor. *Advanced dairy chemistry II*. Amsterdam: Elsevier; 1992. pp 141–190.
2. Sawyer L, Kontopidis G. The core lipocalin, bovine beta-lactoglobulin. *Biochim Biophys Acta* 2000;1482:136–148.
3. Chen WL, Huang MT, Liu HC, Li CW, Mao SJT. Distinction between dry and raw milk using monoclonal antibodies prepared against dry milk proteins. *J Dairy Sci* 2004;87:2720–2729.
4. Song CY, Chen WL, Yang MC, Huang JP, Mao SJT. Epitope mapping of a monoclonal antibody specific to bovine dry milk: involvement of residues 66–76 of strand D in thermal denatured beta-lactoglobulin. *J Biol Chem* 2005;280:3574–3582.
5. Chen WL, Hwang MT, Liao CY, Ho JC, Hong KC, Mao SJT.  $\beta$ -lactoglobulin is a thermal marker in processed milk as studied by electrophoresis and circular dichroic spectra. *J Dairy Sci* 2005;88:1618–1630.
6. Chen WL, Liu WT, Yang MC, Hwang MT, Tsao JH, Mao SJT. A novel conformation-dependent monoclonal antibody specific to the native structure of beta-lactoglobulin and its application. *J Dairy Sci* 2006;89:912–921.
7. Nagaoka S, Futamura Y, Miwa K, Awano T, Yamauchi K, Kanamaru Y, Tadashi K, Kuwata T. Identification of novel hypocholesterolemic peptides derived from bovine milk beta-lactoglobulin. *Biochem Biophys Res Commun* 2001;281:11–17.
8. Zsila F, Bikadi Z, Simonyi M. Retinoic acid binding properties of the lipocalin member beta-lactoglobulin studied by circular dichroism, electronic absorption spectroscopy and molecular modeling methods. *Biochem Pharmacol* 2002;64:1651–1660.
9. Kontopidis G, Holt C, Sawyer L. Invited review: beta-lactoglobulin: binding properties, structure, and function. *J Dairy Sci* 2004;87:785–796.
10. Chevalier F, Chobert JM, Genot C, Haertle T. Scavenging of free radicals, antimicrobial, and cytotoxic activities of the Maillard reaction products of beta-lactoglobulin glycosylated with several sugars. *J Agric Food Chem* 2001;49:5031–5038.
11. Marshall K. Therapeutic applications of whey protein. *Altern Med Rev* 2004;9:136–156.
12. Steinrauf LK. Preliminary X-ray data for some new crystalline forms of  $\beta$ -lactoglobulin and hen-egg-white lysozyme. *Acta Crystallogr* 1959;12:77–79.
13. Aschaffenburg R, Green DW, Simmons RM. Crystal forms of Beta-lactoglobulin. *J Mol Biol* 1965;13:194–201.
14. Green DW, Aschaffenburg R, Camerman A, Coppola JC, Dunnill P, Simmons RM, Komorowski E S, Sawyer L, Turner EM, Woods KE. Structure of bovine beta-lactoglobulin at 6Å resolution. *J Mol Biol* 1979;131:375–397.
15. Papiz MZ, Sawyer L, Eliopoulos EE, North AC, Findlay JB, Sivaprasadarao R, Jones TA, Newcomer ME, Kraulis PJ. The structure of beta-lactoglobulin and its similarity to plasma retinol-binding protein. *Nature* 1986;324:383–385.
16. Monaco HL, Zanotti G, Spadon P, Bolognesi M, Sawyer L, Eliopoulos EE. Crystal structure of the trigonal form of bovine beta-lactoglobulin and of its complex with retinol at 2.5 Å resolution. *J Mol Biol* 1987;197:695–706.
17. Brownlow S, Morais Cabral JH, Cooper R, Flower DR, Yewdall SJ, Polikarpov I, North AC, Sawyer L. Bovine beta-lactoglobulin at 1.8 Å resolution—still an enigmatic lipocalin. *Structure* 1997;5:481–495.
18. Qin BY, Bewley MC, Creamer LK, Baker HM, Baker EN, Jameson GB. Structural basis of the Tanford transition of bovine beta-lactoglobulin. *Biochemistry* 1998;37:14014–14023.
19. Qin BY, Bewley MC, Creamer LK, Baker EN, Jameson GB. Functional implications of structural differences between variants A and B of bovine beta-lactoglobulin. *Protein Sci* 1999;8:75–83.
20. Oliveira KM, Valente-Mesquita VL, Botelho MM, Sawyer L, Ferreira ST, Polikarpov I. Crystal structures of bovine beta-lactoglobulin in the orthorhombic space group C222(1). Structural differences between genetic variants A and B and features of the Tanford transition. *Eur J Biochem* 2001;268:477–483.
21. Adams JJ, Anderson BE, Norris GE, Creamer LK, Jameson GB. Structure of bovine beta-lactoglobulin (variant A) at very low ionic strength. *J Struct Biol* 2006;154:246–254.
22. Sawyer L, Papiz MZ, North ACT, Eliopoulos EE. Structure and function of bovine  $\beta$ -lactoglobulin. *Biochem Soc Trans* 1985;13:265–266.
23. Newcomer ME, Jones TA, Aqvist J, Sundelin J, Eriksson U, Rask L, Peterson PA. The three-dimensional structure of retinol-binding protein. *EMBO J* 1984;3:1451–1454.
24. Redl B. Human tear lipocalin. *Biochim Biophys Acta* 2000;1482:241–248.
25. Kuwata K, Hoshino M, Forge V, Era S, Batt CA, Goto Y. Solution structure and dynamics of bovine beta-lactoglobulin A. *Protein Sci*. 1999;8:2541–2545.
26. Uhrinova S, Smith MH, Jameson GB, Uhrin D, Sawyer L, Barlow PN. Structural changes accompanying pH-induced dissociation of the beta-lactoglobulin dimer. *Biochemistry* 2000;39:3565–3574.
27. Qin BY, Creamer LK, Baker EN, Jameson GB. 12-Bromododecanoic acid binds inside the calyx of bovine beta-lactoglobulin. *FEBS Lett* 1998;438:272–278.
28. Wu SY, Perez MD, Puyol P, Sawyer L. beta-lactoglobulin binds palmitate within its central cavity. *J Biol Chem* 1999;274:170–174.
29. Kontopidis G, Holt C, Sawyer L. The ligand-binding site of bovine beta-lactoglobulin: evidence for a function. *J Mol Biol* 2002;318:1043–1055.

30. Dufour E, Genot C, Haertle T. beta-Lactoglobulin binding properties during its folding changes studied by fluorescence spectroscopy. *Biochim. Biophys. Acta* 1994;1205:105–112.
31. Wang Q, Allen JC, Swaisgood HE. Binding of vitamin D and cholesterol to beta-lactoglobulin. *J Dairy Sci* 1997;80:1054–1059.
32. Wang Q, Allen JC, Swaisgood HE. Binding of retinoids to beta-lactoglobulin isolated by bioselective adsorption. *J Dairy Sci* 1997;80:1047–1053.
33. Wang Q, Allen JC, Swaisgood HE. Protein concentration dependence of palmitate binding to beta-lactoglobulin. *J Dairy Sci* 1998;81:76–81.
34. Wang Q, Allen JC, Swaisgood HE. Binding of lipophilic nutrients to beta-lactoglobulin prepared by bioselective adsorption. *J Dairy Sci* 1999;82:257–264.
35. Muresan S, van der Bent A, de Wolf FA. Interaction of beta-lactoglobulin with small hydrophobic ligands as monitored by fluorometry and equilibrium dialysis: nonlinear quenching effects related to protein–protein association. *J Agric Food Chem* 2001;49:2609–2618.
36. Fessas D, Iametti S, Schiraldi A, Bonomi F. Thermal unfolding of monomeric and dimeric beta-lactoglobulins. *Eur J Biochem* 2001;268:5439–5448.
37. Cogan U, Kopelman M, Mokady S, Shinitzky M. Binding affinities of retinol and related compounds to retinol binding proteins. *Eur J Biochem* 1976;65:71–78.
38. Tseng CF, Lin CC, Huang HY, Liu HC, Mao SJT. Antioxidant role of human haptoglobin. *Proteomics* 2004;4:2221–2228.
39. Otwinowski Z, Minor W. Processing of X-ray Diffraction Data Collected in Oscillation Mode. *Methods Enzymol* 1997;276:307–326.
40. Rossmann MG. The molecular replacement method. *Acta Crystallogr A* 1990;46:73–82.
41. Brunger AT, Adams PD, Clore GM, DeLano WL, Gros P, Grosse-Kunstleve RW, Jiang JS, Kuszewski J, Nilges M, Pannu NS, Read RJ, Rice LM, Simonson T, Warren GL. Crystallography and NMR system: a new software suite for macromolecular structure determination. *Acta Crystallogr D Biol Crystallogr* 1998;54:905–921.
42. Jones TA, Zou JY, Cowan SW, Kjeldgaard Improved methods for building protein models in electron density maps and the location of errors in these models. *Acta Crystallogr A* 1991;47:110–119.
43. Lee SC, Guan HH, Wang CH, Huang WN, Tjong SC, Chen CJ, Wu WG. Structural basis of citrate-dependent and heparan sulfate-mediated cell surface retention of cobra cardiotoxin A3. *J Biol Chem* 2005;280:9567–9577.
44. Covarrubias AS, Bergfors T, Jones TA, Hogbom M. Structural mechanics of the pH-dependent activity of beta-carbonic anhydrase from *Mycobacterium tuberculosis*. *J Biol Chem* 2006;281:4993–4999.
45. Brünger AT. Free R value: a novel statistical quantity for assessing the accuracy of crystal structures. *Nature* 1992;355:472–475.
46. Laskowski RA, MacArthur MW, Moss DS, Thornton JM. PROCHECK: a program to check the stereochemical quality of protein structures. *J Appl Crystallogr* 1993;26:283–291.
47. Engh RA, Huber R. Accurate bond and angle parameters for X-ray protein structure refinement. *Acta Crystallogr A* 1991;47:392–400.
48. Ramachandran GN, Sasisekharan V. Conformation of polypeptides and proteins. *Adv Protein Chem* 1968;23:283–438.
49. Said HM, Ong DE, Shingleton JL. Intestinal uptake of retinol: enhancement by bovine milk beta-lactoglobulin. *Am J Clin Nutr* 1989;49:690–694.
50. Kushibiki S, Hodate K, Kurisaki J, Shingu H, Ueda Y, Watanabe A, Shinoda M. Effect of beta-lactoglobulin on plasma retinol and triglyceride concentrations, and fatty acid composition in calves. *J Dairy Res* 2001;68:579–586.
51. Vieth R. Vitamin D nutrition and its potential health benefits for bone, cancer and other conditions. *J Nutr Environ Med* 2001;11:275–291.
52. Chapuy MC, Arlot ME, Duboeuf F, Brun J, Crouzet B, Arnaud S, Delmas PD, Meunier PJ. Vitamin D<sub>3</sub> and calcium to prevent hip fractures in the elderly women. *N Engl J Med* 1992;327:1637–1642.
53. McKenna MJ, Freaney R, Byrne P, McBrinn Y, Murray B, Kelly M, Donne B, O'Brien M. Safety and efficacy of increasing wintertime vitamin D and calcium intake by milk fortification. *QJM* 1995;88:895–898.
54. Ragona L, Fogolari F, Catalano M, Ugolini R, Zetta L, Molinari H. EF loop conformational change triggers ligand binding in beta-lactoglobulins. *J Biol Chem* 2003;278:38840–38846.
55. Yang J, Powers JR, Clark S, Dunker AK, Swanson BG. Hydrophobic probe binding of beta-lactoglobulin in the native and molten globule state induced by high pressure as affected by pH, KIO(3) and N-ethylmaleimide. *J Agric Food Chem* 2002;50:5207–5214.
56. Makinen-Kiljunen S, Palosuo T. A sensitive enzyme-linked immunosorbent assay for determination of bovine beta-lactoglobulin in infant feeding formulas and in human milk. *Allergy* 1992;47:347–352.
57. Lovegrove JA, Osman DL, Morgan JB, Hampton SM. Transfer of cow's milk beta-lactoglobulin to human serum after a milk load: a pilot study. *Gut* 1993;34:203–207.
58. Saito H, Dhanasekaran P, Nguyen D, Holvoet P, Lund-Katz S, Phillips MC. Domain structure and lipid interaction in human apolipoproteins A-I and E, a general model. *J Biol Chem* 2003;278:23227–23232.
59. Perez MD, Diaz de Villegas C, Sanchez L, Aranda P, Ena JM, Calvo M. Interaction of fatty acids with beta-lactoglobulin and albumin from ruminant milk. *J Biochem* 1989;106:1094–1097.